

# First Evidence for two Different $\mu\text{-}\eta^1\text{-}\eta^1\text{-}$ and $\mu\text{-}\eta^1\text{-}\eta^2\text{-}$ Co-ordination Modes of the $\text{P}_3\text{C}_2\text{Bu}_2$ Ring of $[\text{Fe}(\eta^5\text{-P}_3\text{C}_2\text{Bu}_2)(\eta^5\text{-C}_5\text{H}_5)]$ to a Same Cluster Fragment: Synthesis and Characterisation of $[\text{Ir}_4(\text{CO})_{10}\{[\text{Fe}(\eta^5\text{-P}_3\text{C}_2\text{Bu}_2)(\eta^5\text{-C}_5\text{H}_5)]\}]$ and X-ray Molecular Structure of the $\mu\text{-}\eta^1\text{-}\eta^2\text{-}$ Isomer

Maria Helena Araujo<sup>a,b</sup>, Peter B. Hitchcock<sup>a</sup>, John F. Nixon<sup>\*a</sup> and Maria D. Vargas<sup>\*b</sup>

<sup>a</sup>School of Chemistry, Physics and Environmental Science, University of Sussex, Brighton, BN1 9QJ, UK.

<sup>b</sup>Instituto de Química, Universidade Estadual de Campinas, CP 6154, 13083-970, Campinas - SP, Brazil.

A investigação das estruturas em solução dos compostos  $[\text{Ir}_4(\text{CO})_{11}\text{L}]$  [ $\text{L} = [\text{Fe}(\eta^5\text{-P}_3\text{C}_2\text{Bu}_2)(\eta^5\text{-C}_5\text{H}_5)]$  (**1**) e  $[\text{Fe}(\eta^5\text{-P}_3\text{C}_2\text{Bu}_2)(\eta^5\text{-P}_2\text{C}_3\text{Bu}_3)]$  (**2**)], por espectroscopia de RMN de  $^{13}\text{C}$  e de  $^{31}\text{P}$ , mostrou que, a 163 K, o composto **1** existe na forma de dois isômeros, um deles contendo carbonilas em ponte e o outro, carbonilas terminais, na razão de 1:0,15, respectivamente, enquanto que o composto **2** existe somente na forma do isômero contendo carbonilas em ponte. À temperatura ambiente, somente no composto **2** ocorre um deslocamento 1,2 do anel  $\eta^5\text{-P}_3\text{C}_2\text{Bu}_2$ . Enquanto o composto **2** sofre fácil dissociação de CO em solução para dar  $[\text{Ir}_4(\text{CO})_{10}\{\mu\text{-}\eta^1\text{-}\eta^1\text{-}[\text{Fe}(\eta^5\text{-P}_3\text{C}_2\text{Bu}_2)(\eta^5\text{-P}_2\text{C}_3\text{Bu}_3)]\}]$  (**3**), foi necessário usar  $\text{Me}_3\text{NO}$  para produzir  $[\text{Ir}_4(\text{CO})_{10}\{[\text{Fe}(\eta^5\text{-P}_3\text{C}_2\text{Bu}_2)(\eta^5\text{-C}_5\text{H}_5)]\}]$  (**4**) a partir de **1**. Este composto foi obtido sob a forma de dois isômeros interconversíveis, **4a** e **4b**, que não puderam ser separados. Um estudo de difração de raios-X do isômero **4a** mostrou que o ligante  $[\text{Fe}(\eta^5\text{-P}_3\text{C}_2\text{Bu}_2)(\eta^5\text{-C}_5\text{H}_5)]$  encontra-se ligado em ponte a uma das arestas do tetraedro de  $\text{Ir}_4$ , interagindo através do par de elétrons livres de um dos átomos de fósforo adjacentes e de modo  $\eta^2\text{-}$  através da ligação dupla  $\text{P}=\text{P}$  do anel  $\eta^5\text{-P}_3\text{C}_2\text{Bu}_2$  e que todos os ligantes CO encontram-se ligados de modo terminal. Um estudo de RMN de  $^{31}\text{P}\{^1\text{H}\}$  a várias temperaturas evidenciou um processo fluxional que envolve as interações entre os átomos de  $\text{Ir}_1$  e  $\text{Ir}_2$  e o par de elétrons livres no átomo  $\text{P}_1$ , a ligação  $\text{P}_1\text{-P}_2$  e o par de elétrons livres no átomo  $\text{P}_2$ . De acordo com os dados de RMN multinuclear, a estrutura do cluster **4b** é semelhante à do composto **3**, com o anel  $\eta^5\text{-P}_3\text{C}_2\text{Bu}_2$  coordenado de modo  $\eta^1\text{-}\eta^1\text{-}$  através dos dois átomos de P adjacentes e com todos os ligantes CO ligados de modo terminal.

Investigation of the solution structures of  $[\text{Ir}_4(\text{CO})_{11}\text{L}]$  ( $\text{L} = [\text{Fe}(\eta^5\text{-P}_3\text{C}_2\text{Bu}_2)(\eta^5\text{-C}_5\text{H}_5)]$  (**1**) and  $[\text{Fe}(\eta^5\text{-P}_3\text{C}_2\text{Bu}_2)(\eta^5\text{-P}_2\text{C}_3\text{Bu}_3)]$  (**2**) by  $^{13}\text{C}$  and  $^{31}\text{P}$  NMR spectroscopy showed that, at 163K, **1** exists in the form of two isomers with bridged and non-bridged structures, in a 1:0.15 ratio, respectively, whereas **2** exists only in the bridged form. At RT, 1,2 shift of the  $\eta^5\text{-P}_3\text{C}_2\text{Bu}_2$  ring was only observed for compound **2**. Whereas **2** loses CO readily in solution to give  $[\text{Ir}_4(\text{CO})_{10}\{\mu\text{-}\eta^1\text{-}\eta^1\text{-}[\text{Fe}(\eta^5\text{-P}_3\text{C}_2\text{Bu}_2)(\eta^5\text{-P}_2\text{C}_3\text{Bu}_3)]\}]$  (**3**), activation with  $\text{Me}_3\text{NO}$  was necessary to produce  $[\text{Ir}_4(\text{CO})_{10}\{[\text{Fe}(\eta^5\text{-P}_3\text{C}_2\text{Bu}_2)(\eta^5\text{-C}_5\text{H}_5)]\}]$  (**4**), obtained in the form of two non-interconverting isomers **4a** and **4b**, which were not able to be separated. A single crystal X-ray diffraction study of isomer **4a** established that the  $[\text{Fe}(\eta^5\text{-P}_3\text{C}_2\text{Bu}_2)(\eta^5\text{-C}_5\text{H}_5)]$  ligand bridges one of the edges of the  $\text{Ir}_4$  tetrahedron, interacting *via* the lone electron pair of one of the adjacent P atoms and in an  $\eta^2\text{-}$  mode *via* the P-P double bond of the  $\eta^5\text{-P}_3\text{C}_2\text{Bu}_2$  ring and that all CO ligands are terminally bonded. Variable temperature  $^{31}\text{P}\{^1\text{H}\}$  NMR spectroscopy evidenced a fluxional process involving interactions between the  $\text{Ir}_1$  and  $\text{Ir}_2$  atoms and the lone pair on  $\text{P}_1$ , the  $\text{P}_1\text{-P}_2$  bond, and the lone pair on  $\text{P}_2$ . According to multinuclear NMR, cluster **4b** has similar structure to compound **3**, with the  $\eta^5\text{-P}_3\text{C}_2\text{Bu}_2$  ring coordinated in a  $\eta^1\text{-}\eta^1\text{-}$  mode *via* the two adjacent P atoms, and all CO ligands bonded terminally.

**Keywords:** iridium cluster, fluxional process, tri and pentaphosphaferrocenes

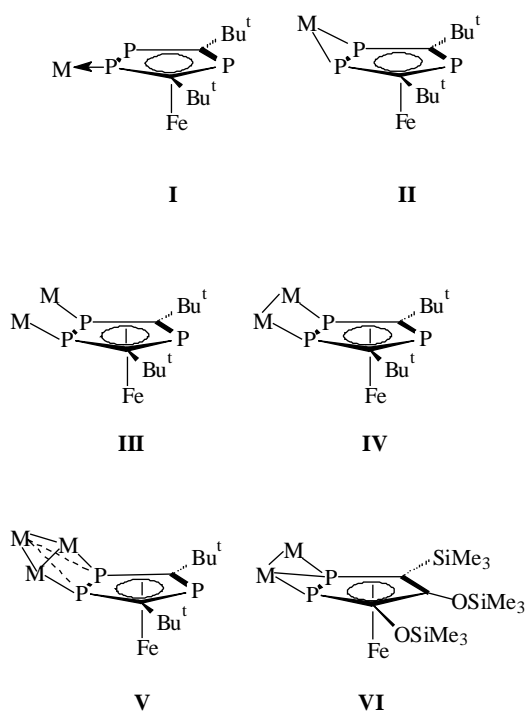
## Introduction

Tri-, penta- and hexaphosphorus analogues of ferrocene

ligands  $[\text{Fe}(\eta^5\text{-P}_3\text{C}_2\text{Bu}_2)(\eta^5\text{-R})]$  ( $\text{R} = \text{P}_2\text{C}_3\text{Bu}_3, \text{P}_3\text{C}_2\text{Bu}_2$  and  $\text{C}_5\text{R}'_5$ ,  $\text{R}' = \text{H}$  or Me) have been reported in recent years<sup>1</sup>. To date two types of co-ordination modes of these phosphoferrocene ligands, I and II, have been reported in the literature, as illustrated below.

\*e-mail: mdvargas@iqm.unicamp.br

Bonding mode I, consisting of  $\eta^1$ -co-ordination *via* the phosphorus lone pair of one of the adjacent P atoms, was observed in several species, *e.g.*  $[\text{M}(\text{CO})_5\{\eta^1\text{-}[\text{Fe}(\eta^5\text{-P}_3\text{C}_2\text{Bu}^t_2)(\eta^5\text{-C}_5\text{R}_5)]\}]$  ( $\text{R} = \text{H}$ ,  $\text{M} = \text{W}$ ;  $\text{R} = \text{Me}$ ,  $\text{M} = \text{Mo}$ ,  $\text{W}$  or  $\text{Cr}$ )<sup>2,3,4</sup> and  $[\text{W}(\text{CO})_5\{\eta^1\text{-}[\text{Fe}(\eta^5\text{-P}_3\text{C}_2\text{Bu}^t_2)(\eta^5\text{-R})]\}]$  ( $\text{R} = \text{P}_2\text{C}_3\text{Bu}^t_3$  or  $\text{P}_3\text{C}_2\text{Bu}^t_2$ )<sup>5</sup>, whereas bonding mode II, involving  $\eta^2$ -ring edge ligation through the P-P multiple bond was only found in  $[\text{Rh}(\eta^5\text{-C}_5\text{Me}_5)\text{CO}\{\eta^2\text{-}[\text{Fe}(\eta^5\text{-P}_3\text{C}_2\text{Bu}^t_2)(\eta^5\text{-C}_5\text{H}_5)]\}]$ <sup>6</sup>. Although the interactions of dinuclear and cluster compounds with phosphaferrrocenes have been much less investigated, their additional bonding capabilities have led to a number of other modes of interactions as shown below.



Thus, bonding mode I, found in  $[\text{Ru}_3(\text{CO})_{11}\{\eta^1\text{-}[\text{Fe}(\eta^5\text{-P}_3\text{C}_2\text{Bu}^t_2)(\eta^5\text{-C}_5\text{Me}_5)]\}]$ <sup>7</sup>, was also observed in  $[\text{Ru}_3(\text{CO})_{10}\{\mu\text{-}\eta^1\text{-}\eta^1\text{-}[\text{Fe}(\eta^5\text{-P}_3\text{C}_2\text{Bu}^t_2)_2]\}]$ <sup>8</sup> in which the two rings co-ordinate to adjacent ruthenium atoms. Bonding modes III and IV in which both lone pairs on adjacent P ring atoms are used was encountered in  $[\text{Ni}(\text{CO})_2\{\eta^1\text{-}\eta^1\text{-}[\text{Fe}(\eta^5\text{-P}_3\text{C}_2\text{Bu}^t_2)(\eta^5\text{-C}_5\text{Me}_5)]\}]$ <sup>4</sup> and  $[\text{Ir}_4(\text{CO})_{10}\{\mu\text{-}\eta^1\text{-}\eta^1\text{-}[\text{Fe}(\eta^5\text{-P}_3\text{C}_2\text{Bu}^t_2)(\eta^5\text{-P}_2\text{C}_3\text{Bu}^t_3)]\}]$  (**3**)<sup>9</sup>, respectively. Bonding mode V of two adjacent P atoms to three metal centres involving symmetrical side-on and end-on co-ordination has only been observed in  $[\text{Ru}_3(\text{CO})_9\{\mu\text{-}\eta^2\text{-}[\text{Fe}(\eta^5\text{-P}_3\text{C}_2\text{Bu}^t_2)(\eta^5\text{-C}_5\text{Me}_5)]\}]$ <sup>7</sup>, and bonding mode VI, involving an asymmetric  $\mu\text{-}\eta^1\text{-}\eta^2$ - interaction of two adjacent P atoms, was reported for  $[\text{Fe}_2(\text{CO})_7\{\mu\text{-}\eta^1\text{-}\eta^2\text{-}[\text{Fe}(\eta^5\text{-P}_2\text{C}_3(\text{OSiMe}_3)_2(\text{SiMe}_3)(\eta^5\text{-C}_5\text{H}_3\text{Bu}^t_2)]\}]$ <sup>10</sup>.

We recently described the  $\text{Ir}_4$  mono-substituted derivatives  $[\text{Ir}_4(\text{CO})_{11}\text{L}]$  [ $\text{L} = [\text{Fe}(\eta^5\text{-P}_3\text{C}_2\text{Bu}^t_2)(\eta^5\text{-C}_5\text{H}_5)]$  (**1**) and  $[\text{Fe}(\eta^5\text{-P}_3\text{C}_2\text{Bu}^t_2)(\eta^5\text{-P}_2\text{C}_3\text{Bu}^t_3)]$  (**2**)] which were isolated in yields up to 90 % from  $\text{NBu}_4[\text{Ir}_4(\text{CO})_{11}\text{Br}]$  by bromide abstraction with silver salts in the presence of  $\text{L}^9$ . Their <sup>31</sup>P NMR spectra were particularly informative and established different behaviour in solution. Whereas at room temperature the pentaphosphaferrocene derivative **2** exhibited a rapid 1,2 shift of the  $\text{Ir}_4$  fragment between adjacent P atoms, as previously observed for  $[\text{W}(\text{CO})_5\{\eta^1\text{-}[\text{M}(\eta^5\text{-P}_3\text{C}_2\text{Bu}^t_2)(\eta^5\text{-P}_2\text{C}_3\text{Bu}^t_3)]\}]$  ( $\text{M} = \text{Fe}$  or  $\text{Ru}$ )<sup>11</sup>, the room temperature spectrum of the triphosphaferrocene species **1** revealed the three different environments of the P-ring atoms. Furthermore, compound **2** was shown to undergo facile CO dissociation in solution with formation of  $[\text{Ir}_4(\text{CO})_{10}\{\mu\text{-}\eta^1\text{-}\eta^1\text{-}[\text{Fe}(\eta^5\text{-P}_3\text{C}_2\text{Bu}^t_2)(\eta^5\text{-P}_2\text{C}_3\text{Bu}^t_3)]\}]$  (**3**). Under similar conditions, however, the analogous compound **1** was found to be stable. These structural and reactivity differences were rationalised in terms of the slightly different basicities of the two phosphaferrrocene ligands. In this paper we describe the  $\text{Me}_3\text{NO}$  induced transformation of compound **1** into two isomers of  $[\text{Ir}_4(\text{CO})_{10}\{\text{Fe}(\eta^5\text{-P}_3\text{C}_2\text{Bu}^t_2)(\eta^5\text{-C}_5\text{H}_5)\}]$  (**4a** and **4b**) in which the  $[\text{Fe}(\eta^5\text{-P}_3\text{C}_2\text{Bu}^t_2)(\eta^5\text{-C}_5\text{H}_5)]$  ligand exhibits different co-ordination modes VI and IV, respectively. We also present further solution characterisation of compounds **1**, **2** and **3** by NMR spectroscopy.

## Results and Discussion

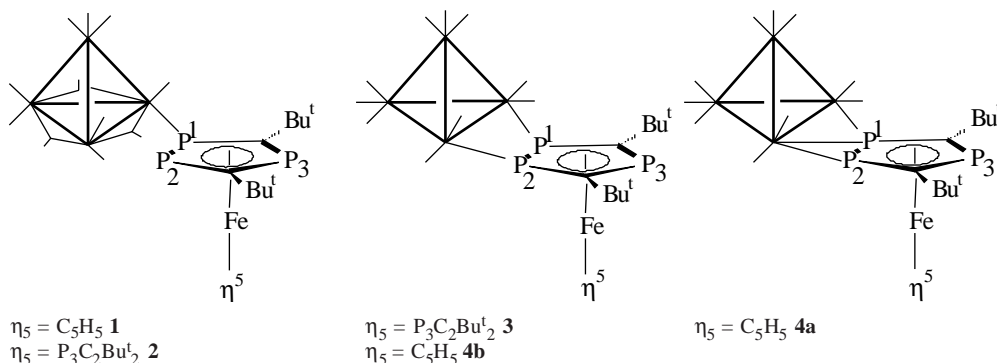
### *Synthesis of $[\text{Ir}_4(\text{CO})_{10}\{\text{Fe}(\eta^5\text{-P}_3\text{C}_2\text{Bu}^t_2)(\eta^5\text{-C}_5\text{H}_5)\}]$ (**4a** and **4b**)*

Thermolysis of the triphosphaferrocene derivative **1** in toluene at 60 °C for 48 h did not lead to the product analogous to the known species **3**. Activation of dark orange compound **1** was only achieved by treatment with an equivalent amount of  $\text{Me}_3\text{NO}$ , at -78 °C, in  $\text{CH}_2\text{Cl}_2$  and then by allowing the solution to warm up slowly to room temperature. The resulting brown product (78% yield after purification by TLC) was later identified by <sup>31</sup>P{<sup>1</sup>H} NMR spectroscopy to be a mixture of two isomeric forms of the expected product (**4a**:**4b** ~1:0.07). These isomers only differ slightly with respect to the co-ordination mode of the triphosphaferrocene and could not be separated by TLC under a variety of conditions. The mixture was characterised by analytical and spectroscopic data (Table 1 and Experimental). Crystals of isomer **4a** were obtained from  $\text{CH}_2\text{Cl}_2$ /hexane at 4 °C and a single crystal X-ray analysis was carried out.

**Table 1.**  $^{31}\text{P}\{^1\text{H}\}$  and  $^{13}\text{C}\{^1\text{H}\}$  NMR data for compounds **1**, **2**, **3**, **4a** and **4b**.

Compound	$^{31}\text{P}\{^1\text{H}\}$ NMR	$^{13}\text{C}\{^1\text{H}\}$ NMR
<b>1</b> (maj. isom.)	-18.3 [d, P <sub>1</sub> , $^1J(\text{P}_1\text{P}_2)$ 457] 8.9 (d, P <sub>2</sub> ), 16.7 (s, P <sub>3</sub> )	205.0 (1CO), 204.4 (1CO), 195.3 (1CO), 173.6 (1CO), 171.2 (1CO), 170.0 (1CO), 156.7 (1CO), 156.4 (1CO), 155.8 (1CO), 153.9 (2CO), 163.2 (1CO), 159.6 (1CO), 159.1 (1CO),
	(min. isom.)	158.1 (1CO), 156.8 (1CO), 156.0 (1CO), 155.7 (2CO), 154.7 (1CO), 154.1 (1CO), 153.4 (1CO)
<b>2</b>	-15.0 (dd, P <sub>1</sub> ) $^1J(\text{P}_1\text{P}_2)$ 445.6, $^1J(\text{P}_1\text{P}_3)$ 42.7] 9.9 [dd, P <sub>2</sub> , $^2J(\text{P}_2\text{P}_3)$ 34.3] 8.8 (t, P <sub>3</sub> ), 43.0 [d, P <sub>4</sub> , $^2J(\text{P}_4\text{P}_5)$ 41.2] 46.6 (d, P <sub>5</sub> )	205.9 (1CO), 201.9 (1CO), 195.3 (1CO), 173.2 (2CO), 169.2 (1CO), 158.8 (1CO), 155.6 (1CO), 154.9 (d, 1CO, J(PC) 44.4), 154.3 (1CO), 152.2 (1CO)
<b>3</b>	-142.0 [d, P <sub>1</sub> , P <sub>2</sub> , $^2J(\text{P}_1, \text{P}_2\text{P}_3)$ 41.0] 31.7 (t, P <sub>3</sub> ) 39.5 (s, P <sub>4</sub> , P <sub>5</sub> )	169.0 (1CO), 167.1 (1CO), 165.8 (2CO), 162.3 (1CO), 157.0 (1CO), 156.0 (1CO), 155.6 (1CO), 154.0 (2CO)
<b>4a</b>	140.0 [dd, P <sub>1</sub> , $^1J(\text{P}_1\text{P}_2)$ 351.0] -148.0 [dd, P <sub>2</sub> , $^2J(\text{P}_2\text{P}_3)$ 24.5] 55.0 [t, P <sub>3</sub> , $^2J(\text{P}_3\text{P}_1)$ 44.6]	172.3 (1CO), 170.1 (1CO), 167.7 (1CO), 161.5 (1CO), 159.4 (2CO), 158.6 (2CO), 158.4 (1CO), 155.4 (1CO)
<b>4b</b>	25.0 (t, P <sub>3</sub> ), -174.0 [d, P <sub>1</sub> P <sub>2</sub> , $^2J(\text{P}_1, \text{P}_2\text{P}_3)$ 37.0]	

Chemical shifts ( $\delta$ ) in ppm and coupling constants ( $J$ ) in Hz. Measured in  $\text{CD}_2\text{Cl}_2/\text{CS}_2$  at  $-105^\circ\text{C}$ .



#### Molecular structure of $[\text{Ir}_4(\text{CO})_{10}\{\text{Fe}(\eta^5\text{-P}_3\text{C}_2\text{Bu}^t_2)(\eta^5\text{-C}_5\text{H}_5)\}]$ (**4a**)

The molecular structure of compound **4a** is shown in Figure 1. Selected bond lengths and angles are given in Table 2.

The structure confirms the bonding mode of the  $\eta^5\text{-P}_3\text{C}_2\text{Bu}^t_2$  ring to the cluster proposed on the basis of the  $^{31}\text{P}$  NMR data (Table 1) discussed below. The four iridium atoms exhibit a distorted tetrahedral  $\text{Ir}_4$  core with Ir-Ir bond lengths lying in the range 2.665(1)-2.723(1) Å and the longest Ir-Ir edge [Ir(1)-Ir(2) 2.723(1) Å] spanned asymmetrically by the 4-electron donor  $[\text{Fe}(\eta^5\text{-P}_3\text{C}_2\text{Bu}^t_2)(\eta^5\text{-C}_5\text{H}_5)]$  ligand *via* the two adjacent P atoms. All the carbonyl ligands are terminally bonded. As in the other rare tetrahedral  $\text{Ir}_4$  clusters containing only terminal CO ligands<sup>12-14</sup>, the average Ir-Ir distance of 2.6945 Å is

relatively short, comparable with the average Ir-Ir distance of 2.693 Å in the parent binary carbonyl  $[\text{Ir}_4(\text{CO})_{12}]$ <sup>15</sup>. The Ir-C and C-O bond distances are in the normal range of values found for terminal CO groups. The marked differences in the Ir-P bond lengths [Ir(2)-P(1) 2.252(5) Å, Ir(1)-P(1) 2.455(5) Å and Ir(1)-P(2) 2.517(5) Å] can best be explained in terms of a  $\eta^1$ - interaction of P(1) with Ir(2) and a  $\eta^2$ - interaction of the P(1)-P(2) bond with Ir(1) atom, as described in bonding mode VI. The Ir(2)-P(1) distance is slightly shorter than Ir-P bond lengths found in other triphosphaferrocene containing iridium clusters, *i.e.*  $[\text{Ir}_4(\text{CO})_{11}\{\text{Fe}(\eta^5\text{-P}_3\text{C}_2\text{Bu}^t_2)(\eta^5\text{-C}_5\text{H}_5)\}]$  2.345(4) Å and  $[\text{H}\text{Ir}_4(\text{CO})_{10}\{\{\text{Fe}(\eta^5\text{-P}_3\text{C}(\text{CMe}_2\text{CH}_2)(\text{CBu}^t)(\eta^5\text{-C}_5\text{H}_5)\}[\text{Ir}_4(\text{CO})_{11}]$  [2.230(7) and 2.318(7) Å]<sup>9</sup>, although it is within the values observed in  $\text{Ir}_4$  clusters containing phosphines<sup>9,16,17</sup>. The Fe atom maintains its  $\eta^5$ - interaction with the  $\text{P}_3\text{C}_2\text{Bu}^t_2$  ring [Fe-P(2) 2.350(6) and Fe(3) 2.328(6) Å],

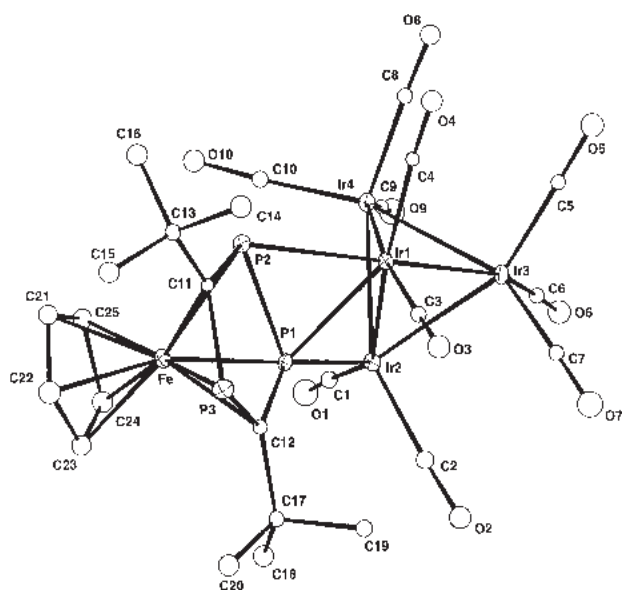


**Figure 1.** Molecular structure of  $[\text{Ir}_4(\text{CO})_{10}\{\text{Fe}(\eta^5\text{-P}_3\text{C}_2\text{Bu}_2)(\eta^5\text{-C}_5\text{H}_5)\}]$  (**4a**).

although the additional  $\eta^2$ -side-on co-ordination of the  $\text{P}_3\text{C}_2\text{Bu}_2$  ring leads to a significant P(1)-P(2) bond lengthening from 2.114(1) Å in the free ligand <sup>6</sup> to 2.268(8) Å in the title compound, as previously observed for the other

complex with similar interaction, *i.e.*  $[\text{Fe}_2(\text{CO})_7\{\mu\text{-}\eta^1\text{-}\eta^2\text{-}[\text{Fe}(\eta^5\text{-P}_2\text{C}_3(\text{OSiMe}_3)_2(\text{SiMe}_3)(\eta^5\text{-C}_5\text{H}_3\text{Bu}^t_2)]\}]^{10}$  [2.281(4) Å] or even for other compounds with analogous types of interaction, *e.g.*  $[\text{Ru}_3(\text{CO})_9\{\mu\text{-}\eta^2\text{-}[\text{Fe}(\eta^5\text{-P}_3\text{C}_2\text{Bu}^t_2)(\eta^5\text{-C}_5\text{Me}_5)]\}]^7$  [2.131(2) Å],  $[\text{Rh}(\eta^5\text{-C}_5\text{Me}_5)(\text{CO})\{\eta^2\text{-}[\text{Fe}(\eta^5\text{-P}_3\text{C}_2\text{Bu}^t_2)(\eta^5\text{-C}_5\text{H}_5)]\}]^6$  [2.306(2) Å] and  $[\text{Ir}(\eta^5\text{-C}_5\text{Me}_5)(\text{CO})\{\eta^2\text{-}[\text{Fe}(\eta^5\text{-P}_5)(\eta^5\text{-C}_5\text{Me}_5)]\}]^{18}$  [2.359(2) Å].

#### Solution behaviour of compounds **3**, **4a**, and **4b**.

A variable temperature  $^{31}\text{P}\{^1\text{H}\}$  NMR study of the mixture containing **4a** and **4b** in  $\text{CD}_2\text{Cl}_2/\text{CS}_2$  (Figure 2) revealed that compound **4a** is fluxional in solution and also established that **4a** and **4b** do not undergo inter-conversion.

At 298 K the P nuclei of **4a** appeared as broad signals at  $\delta$  58 and between  $\delta$  -25 and 25. At 168 K a pattern of lines corresponding to an [AMX] spin system emerged indicating that there were three distinct phosphorus sites (Table 1). The large separation between the  $\text{P}_1$  and  $\text{P}_2$  resonances of 288 ppm and a decrease in the  $^1J(\text{P}_1\text{P}_2)$  from 457 Hz in compound **1** to 351 Hz in **4a** are in accord with the  $^{31}\text{P}$  NMR data reported for  $[\text{Fe}_2(\text{CO})_7\{\mu\text{-}\eta^1\text{-}\eta^2\text{-}[\text{Fe}(\eta^5\text{-P}_2\text{C}_3(\text{OSiMe}_3)_2(\text{SiMe}_3)(\eta^5\text{-C}_5\text{H}_3\text{Bu}^t_2)]\}]^{10}$  for

**Table 2.** Selected bond distances (Å) and angles (deg) for **4a**.

Ir(1)-Ir(3)	2.704(1)	Ir(1)-Ir(4)	2.706(1)	Ir(1)-Ir(2)	2.723(1)
Ir(2)-Ir(3)	2.665(1)	Ir(2)-Ir(4)	2.693(1)	Ir(3)-Ir(4)	2.676(1)
Ir(1)-P(1)	2.455(5)	Ir(1)-P(2)	2.517(5)	Ir(2)-P(1)	2.252(5)
P(1)-P(2)	2.268(8)	Ir(1)-C(3)	1.86(2)	Ir(1)-C(4)	1.92(2)
Ir(2)-C(1)	1.85(2)	Ir(2)-C(2)	1.87(2)	Ir(3)-C(5)	1.90(2)
Ir(3)-C(6)	1.84(2)	Ir(3)-C(7)	1.87(2)	Ir(4)-C(8)	1.90(2)
Ir(4)-C(9)	1.87(2)	Ir(4)-C(10)	1.86(2)	P(1)-C(12)	1.74(2)
P(2)-C(11)	1.77(2)	P(3)-C(11)	1.79(2)	P(3)-C(12)	1.75(2)
C(3)-Ir(1)-C(4)	93.5(9)	C(3)-Ir(1)-P(1)	91.7(7)		
C(4)-Ir(1)-P(1)	148.5(6)	C(3)-Ir(1)-P(2)	102.5(7)		
C(4)-Ir(1)-P(2)	94.3(6)	P(1)-Ir(1)-P(2)	54.3(2)		
C(3)-Ir(1)-Ir(3)	107.9(7)	C(4)-Ir(1)-Ir(3)	98.3(6)		
P(1)-Ir(1)-Ir(3)	109.61(13)	P(2)-Ir(1)-Ir(3)	146.17(12)		
C(3)-Ir(1)-Ir(4)	166.7(9)	C(4)-Ir(1)-Ir(4)	91.6(6)		
P(1)-Ir(1)-Ir(4)	90.04(12)	P(2)-Ir(1)-Ir(4)	89.13(12)		
Ir(3)-Ir(1)-Ir(4)	59.30(3)	C(3)-Ir(1)-Ir(2)	112.3(7)		
C(4)-Ir(1)-Ir(2)	149.2(6)	P(1)-Ir(1)-Ir(2)	51.25(12)		
P(2)-Ir(1)-Ir(2)	96.11(13)	Ir(3)-Ir(1)-Ir(2)	58.83(3)		
Ir(4)-Ir(1)-Ir(2)	59.47(3)	C(1)-Ir(2)-C(2)	99.5(10)		
C(1)-Ir(2)-P(1)	114.4(7)	C(2)-Ir(2)-P(1)	102.9(7)		
C(1)-Ir(2)-Ir(3)	121.2(7)	C(2)-Ir(2)-Ir(3)	93.5(7)		
P(1)-Ir(2)-Ir(3)	117.91(14)	C(1)-Ir(2)-Ir(4)	91.2(7)		
C(2)-Ir(2)-Ir(4)	153.0(7)	P(1)-Ir(2)-Ir(4)	94.90(14)		
Ir(3)-Ir(2)-Ir(4)	59.93(4)	C(1)-Ir(2)-Ir(1)	147.1(7)		
C(2)-Ir(2)-Ir(1)	113.3(7)	P(1)-Ir(2)-Ir(1)	58.23(14)		
Ir(3)-Ir(2)-Ir(1)	60.23(3)	Ir(4)-Ir(2)-Ir(1)	59.95(3)		
C(12)-P(1)-Ir(2)	136.8(8)	Fe-P(1)-Ir(2)	151.7(3)		
C(12)-P(1)-P(2)	100.2(8)	Fe-P(1)-P(2)	62.9(2)		
Ir(2)-P(1)-P(2)	119.2(2)	C(12)-P(1)-Ir(1)	117.4(8)		
Ir(2)-P(1)-Ir(1)	70.5(1)	P(2)-P(1)-Ir(1)	64.3(2)		
C(11)-P(2)-P(1)	94.7(7)	C(11)-P(2)-Ir(1)	114.6(7)		
P(1)-P(2)-Ir(1)	61.5(2)				

which same bonding mode was established in the solid state and in solution. As shown in Figure 3, the lowest chemical shift observed in the spectrum of this iron compound was attributed to  $\text{P}_1$ .

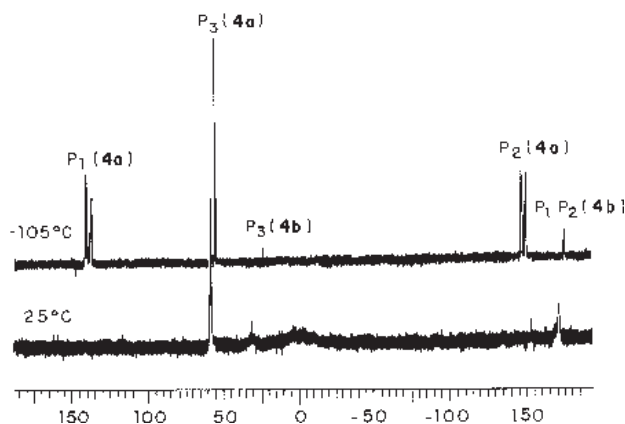


**Figure 2.** VT  $^{31}\text{P}\{^1\text{H}\}$  NMR spectra of the mixture containing compounds **4a** and **4b**.

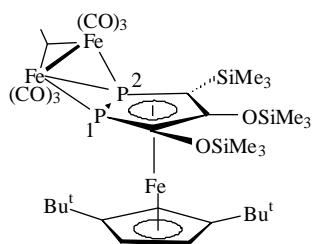


**Figure 3.** Structure of  $[\text{Fe}_2(\text{CO})_7\{\mu\text{-}\eta^1\text{-}\eta^2\text{-}[\text{Fe}(\eta^5\text{-P}_2\text{C}_3(\text{OSiMe}_3)_2(\text{SiMe}_3)(\eta^5\text{-C}_5\text{H}_3\text{Bu}^t_2)]\}]$ ;  $^{31}\text{P}\{^1\text{H}\}$  NMR data:  $\delta$  -162.7 (d,  $\text{P}_1$ ) and  $\delta$  69.2 (d,  $\text{P}_2$ ),  $^1J_{\text{P}_1\text{P}_2}$  276.6 Hz

The fluxional process exhibited by isomer **4a** can be explained in terms of a rapid 1,2 shift of the  $\text{Ir}_1$  and  $\text{Ir}_2$  atoms between  $\text{P}_1$  and the  $\text{P}_1\text{-P}_2$  bond to the adjacent  $\text{P}_2$  and  $\text{P}_1\text{-P}_2$  bond, respectively, as illustrated in Figure 4. It is interesting to note that compound  $[\text{Fe}_2(\text{CO})_7\{\mu\text{-}\eta^1\text{-}\eta^2\text{-}[\text{Fe}(\eta^5\text{-P}_2\text{C}_3(\text{OSiMe}_3)_2(\text{SiMe}_3)(\eta^5\text{-C}_5\text{H}_3\text{Bu}^t_2)]\}]^{10}$  does not exhibit same fluxional behaviour.

The room temperature  $^{31}\text{P}\{^1\text{H}\}$  NMR spectrum of the mixture indicated that compound **4b** (Figure 2 and Table 1) is very similar to  $[\text{Ir}_4(\text{CO})_{10}\{\text{Fe}(\eta^5\text{-P}_3\text{C}_2\text{Bu}^t_2)(\eta^5\text{-P}_2\text{C}_3\text{Bu}^t_3)\}]$  **3**<sup>9</sup>. It shows the equivalence of the two adjacent phosphorus nuclei of the  $\eta^5\text{-P}_3\text{C}_2\text{Bu}^t_2$  ring,  $\text{P}_1$  and  $\text{P}_2$ , which appear as a doublet at relatively low frequency, thus indicating that the  $[\text{Fe}(\eta^5\text{-P}_3\text{C}_2\text{Bu}^t_2)(\eta^5\text{-C}_5\text{H}_5)]$  ligand is co-ordinated to the  $\text{Ir}_4$  fragment *via* these two P atoms, as described in bonding mode IV. It is interesting that neither compound **4b** nor compound **3** exhibit fluxionality of the phosphapherrocene ligand.

In the  $^{13}\text{C}\{^1\text{H}\}$  NMR spectrum of the mixture of **4a** and

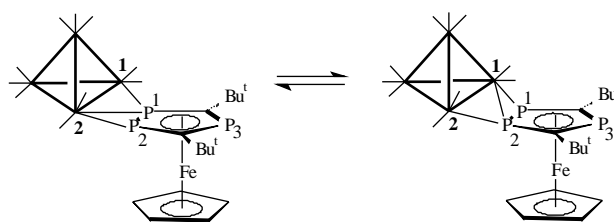


**Figure 4.** Proposed mechanism for the fluxional process in **4a**.

**4b** containing  $^{13}\text{CO}$  enriched carbonyl ligands in  $\text{CD}_2\text{Cl}_2/\text{CS}_2$ , at 168K, (Table 1) only signals due to terminal carbonyls of compound **4a** were observed. Therefore the ground state geometry of isomer **4a** is similar to the structure in the solid state. Due to the very low concentration of isomer **4b** in the mixture, it was not possible to identify all carbonyl resonances of this isomer in the  $^{13}\text{C}\{^1\text{H}\}$  NMR spectra of the mixture, even at 168 K. An indication that this compound contains only terminal CO ligands came from the IR spectrum of the **4a** and **4b** mixture in hexane (Experimental), which only exhibited terminal  $\nu_{\text{CO}}$  bands, and also from the  $^{13}\text{C}\{^1\text{H}\}$  NMR spectra of the analogous  $^{13}\text{CO}$  enriched **3**. At room temperature, broad resonances between  $\delta$  170 and 155 could be spotted, but upon cooling the  $\text{CD}_2\text{Cl}_2/\text{CS}_2$  solution of **3** to 168K, the 10 resonances due to terminal CO ligands were observed (Table 1).

The fact that in solution all three compounds **3**, **4a**, and **4b** have a ground state geometry with all CO ligands terminal is rather interesting and merits a few considerations. Indeed, all  $[\text{Ir}_4(\text{CO})_{10}(\mu\text{-L-L})]$  clusters (L-L = diphosphine ligands) known to date exhibit the alternative ground state geometry with three edge bridging COs defining the basal plane of the metal tetrahedron<sup>13,19</sup>. As has been pointed out before<sup>12</sup>, the derivatives with unbridged structure always exhibit shorter Ir-Ir bonds than those with bridged structure. Consequently it might be that formation of a four-membered Ir-Ir-P-P ring upon coordination of the adjacent P atoms of the phosphapherrocene ligand in compounds **3** and **4a** leads to a preference for the structure with short Ir-Ir bonds over the alternative bridged structure, whereas generation of larger rings with five or more members in diphosphine containing clusters might be responsible for the stabilisation of the bridged structure. Ring size is certainly not the only determining factor in the stabilisation of one of these structures over the other. Indeed, although co-ordination of L-L =  $\text{Ph}_2\text{PC}(\text{H})\text{MePPh}_2$  and  $\text{MeSC}(\text{H})\text{MeSMe}$  in  $[\text{Ir}_4(\text{CO})_{10}(\mu\text{-L-L})]$  generates five-membered rings in both cases, X-ray diffraction and VT  $^{13}\text{C}$  NMR studies have established that the diphosphine compound exhibits the bridged structure, whereas the dithioethane derivative has the alternative unbridged structure, both in solution and in the solid state<sup>14</sup>.



### Solution characterisation of compounds **1** and **2**.

In our previous paper<sup>9</sup> we reported that the solid-state structure of compound **1** exhibited only terminally bonded carbonyl ligands. However, its solution IR showed the presence of terminal and bridging CO ligands, implying that this compound existed as a mixture of the bridging and non-bridging isomers. A VT  $^31\text{P}\{^1\text{H}\}$  NMR study indicated that the  $[\text{Fe}(\eta^5\text{-P}_3\text{C}_2\text{Bu}^t_2)(\eta^5\text{-C}_5\text{H}_5)]$  ligand was not fluxional at room temperature and that at 165 K, the two isomers were present in solution in a 1:0.15 ratio.

In order to find out which was the highest concentration isomer, a variable-temperature  $^{13}\text{C}\{^1\text{H}\}$  NMR study of an enriched  $^{13}\text{CO}$  sample of compound **1** was undertaken in  $\text{CD}_2\text{Cl}_2/\text{CS}_2$ . At room temperature, broad resonances between  $\delta$  170-165 and  $\delta$  158-155 and a singlet at  $\delta$  154 were observed, indicating fluxionality of the CO ligands. As shown in Table 1, the spectrum obtained at 165K exhibited the eleven resonances of the two isomers and established that the predominant isomer in solution is the bridging isomer.

In contrast, the low temperature  $^{13}\text{C}\{^1\text{H}\}$  NMR spectrum of an enriched  $^{13}\text{CO}$  sample of compound **2** (Table 1) only showed the presence of eleven CO ligands of the bridging isomer, thus indicating that this compound exists in solution only in the bridging form.

### Conclusions

It is clear that the nature of the  $\eta^5\text{-C}_5\text{H}_5$  and  $\eta^5\text{-P}_2\text{C}_3\text{Bu}^t_3$  rings in the  $L = [\text{Fe}(\eta^5\text{-P}_3\text{C}_2\text{Bu}^t_2)(\eta^5\text{-C}_5\text{H}_5)]$  and  $[\text{Fe}(\eta^5\text{-P}_3\text{C}_2\text{Bu}^t_2)(\eta^5\text{-P}_2\text{C}_3\text{Bu}^t_3)]$  ligands, respectively, influences markedly: i) the relative stabilities of the  $[\text{Ir}_4(\text{CO})_{11}L]$  compounds and the activation energies for the 1,2 shift of the  $\text{P}_3\text{C}_2\text{Bu}^t_2$  ring in the two species, the pentaphosphaferrocene derivative **2** being far more labile and reactive than cluster **1**, and in a subtle way, the CO ligands distribution in the co-ordination sphere of these clusters, and ii) the mode of interaction of the  $\text{P}_3\text{C}_2\text{Bu}^t_2$  ring in the  $[\text{Ir}_4(\text{CO})_{10}(\mu\text{-L})]$  clusters. Our results suggest that the  $\eta^5\text{-C}_5\text{H}_5$  ring exerts an inductive effect on the  $\eta^5\text{-P}_3\text{C}_2\text{Bu}^t_2$  ring, rendering the  $[\text{Fe}(\eta^5\text{-P}_3\text{C}_2\text{Bu}^t_2)(\eta^5\text{-C}_5\text{H}_5)]$  ligand more basic than the pentaphosphaferrocene ligand, which explains the higher activation energy needed for CO loss for **1**, compared to **2**, and also the fact that electronic density along the P-P bond in  $[\text{Fe}(\eta^5\text{-P}_3\text{C}_2\text{Bu}^t_2)(\eta^5\text{-C}_5\text{H}_5)]$  becomes available for co-ordination and competes with the lone pairs of the adjacent P atoms. Thus, whereas in compound **3** the pentaphosphaferrocene ligand co-ordinates *via* the adjacent P lone pairs in a  $\eta^1\text{-}\eta^1$ - mode, in the main product (1:0.07)

from CO loss in **1**, **4a**, the  $\text{P}_3\text{C}_2\text{Bu}^t_2$  ring interacts in a  $\eta^1\text{-}\eta^2$ - mode.

### Experimental

All manipulations and reactions were performed under an atmosphere of dry argon, unless otherwise specified, by using Schlenk-type glassware, syringe and high vacuum-line techniques, with glassware dried in vacuum prior to use. Solvents were dried, degassed and redistilled before use,  $\text{CH}_2\text{Cl}_2$  was dried over  $\text{CaH}_2$ , hexane over sodium wire and thf over sodium and benzophenone. The compound  $[\text{Ir}_4(\text{CO})_{11}\{\text{Fe}(\eta^5\text{-P}_3\text{C}_2\text{Bu}^t_2)(\eta^5\text{-C}_5\text{H}_5)\}]$  **1** was prepared as described previously<sup>9</sup>, and  $\text{Me}_3\text{NO}\cdot 3\text{H}_2\text{O}$  was sublimed in vacuum. Purification of the products was carried out by preparative TLC (1 mm thickness glass-backed silica plates 20 x 20 cm, silica gel type GF<sub>254</sub>, Fluka) using  $\text{CH}_2\text{Cl}_2$ /hexane (1:4 v/v) as eluent and the compound was extracted from silica with  $\text{CH}_2\text{Cl}_2$ . Compounds  $[\text{Fe}(\eta^5\text{-P}_3\text{C}_2\text{Bu}^t_2)(\eta^5\text{-C}_5\text{H}_5)]$ <sup>6</sup> and  $[\text{Fe}(\eta^5\text{-P}_3\text{C}_2\text{Bu}^t_2)(\eta^5\text{-P}_2\text{C}_3\text{Bu}^t_3)]$ <sup>20</sup> were synthesised according to the literature. Samples of  $^{13}\text{CO}$  enriched clusters, prepared from  $\text{NBu}_4[\text{Ir}_4(\text{CO})_{11}\text{Br}]$ <sup>21</sup>, were used for the  $^{13}\text{C}$  NMR experiments. All  $\text{Ir}_4$ -clusters were stored under an inert atmosphere to avoid decomposition observed in some of the compounds stored for long time in the solid state.

Solution NMR spectra were recorded on a Bruker DPX 300 or AC 300P. Standard pulse sequences were used for the NMR experiments. They were carried out in  $\text{CD}_2\text{Cl}_2/\text{CS}_2$  ( $\text{CS}_2$   $\delta$  191.75) solutions. Chemical shifts are given in ppm and coupling constants (*J*) in Hz. Deuterated solvents were used as lock and reference ( $^1\text{H}$  NMR relative to the proton resonance resulting from incomplete deuteration of the  $\text{CD}_2\text{Cl}_2$  (5.32);  $^{13}\text{C}$  NMR relative to the carbon of the  $\text{CD}_2\text{Cl}_2$  (53.7) and for  $^{31}\text{P}$  NMR external 85 %  $\text{H}_3\text{PO}_4$ ). Infrared spectra were recorded on a Bomem (FT-IR Michelson) spectrophotometer scanning between 2200 and 1600  $\text{cm}^{-1}$  ( $\nu_{\text{CO}}$ ) using a  $\text{CaF}_2$  liquid cell.

### Synthesis of $[\text{Ir}_4(\text{CO})_{10}\{\text{Fe}(\eta^5\text{-C}_5\text{H}_5)(\eta^5\text{-P}_3\text{C}_2\text{Bu}^t_2)\}]$ **4a** and **4b**.

An orange solution of **1** (200 mg, 0.14 mmol) in  $\text{CH}_2\text{Cl}_2$  (30 mL) was cooled to -78 °C and treated with a  $\text{CH}_2\text{Cl}_2$  solution (2 mL) of  $\text{Me}_3\text{NO}$  (10.5 mg, 0.14 mmol). The reaction mixture was allowed to warm to room temperature, and the solution concentrated *in vacuo*. Separation of the products by TLC afforded **4a** and **4b** as a mixture (150 mg, 0.11 mmol, 78 %) and unreacted **1** (30 mg, 0.02 mmol, 14 %) along with some decomposition (base line on the TLC plates). IR  $\nu_{\text{max}}/\text{cm}^{-1}$  (CO) 2085.2vs, 2053.5vs, 2034.7vs, 2027.8vs, 2006.7m, 1991.2s and 1968.3m (hexane).

$^1\text{H-NMR}$  (25 °C, 300 MHz): **4a**  $\delta$  4.9 (s, 5H, Cp) and 1.6 (s, 18H,  $^t\text{Bu}$ ); **4b**  $\delta$  5.2 (s, 5H, Cp) and 1.2 (s, 18H,  $^t\text{Bu}$ ).

#### Solution characterization of **1**.

$^{13}\text{C}\{^1\text{H}\}$ -NMR spectrum except CO region (25 °C, 75.43 MHz):  $\delta$  76.1 (s, 5C, Cp), 38.8 [dd, 1C,  $^2J(\text{CP})$  17.4,  $^3J(\text{CP})$  5.8 Hz,  $\text{CMe}_3$ ], 38.3 [dd, 1C,  $^2J(\text{CP})$  15.3,  $^3J(\text{CP})$  4.4 Hz,  $\text{CMe}_3$ ], 35.8 [dd, 3C,  $^3J(\text{CP})$  10.9,  $^3J(\text{CP})$  4.4 Hz,  $\text{CCH}_3$ ], 35.5 [t, 3C,  $^3J(\text{CP})$  9.4 Hz,  $\text{CCH}_3$ ].

#### Crystallographic data for **4a**.

$\text{C}_{25}\text{H}_{23}\text{FeIr}_4\text{O}_{10}\text{P}_3$ ;  $M = 1401.0$ ; monoclinic; space group  $\text{P}2_1/\text{n}$ ;  $a = 9.779(2)$ ,  $b = 14.396(5)$ ,  $c = 22.783(6)$  Å;  $\beta = 96.32(2)^\circ$ ;  $U = 3188(2)$  Å $^3$ ;  $Z = 4$ ;  $D_{\text{calc.}} = 2.92$  Mg/m $^3$ ; crystal dimensions 0.4 x 0.4 x 0.3 mm;  $F(000) = 2528$ ;  $T = 173(2)$  K; Mo-K $\alpha$  radiation  $\lambda = 0.71073$  Å. Data were collected on an Enraf-Nonius CAD4 diffractometer and of the total 5331 independent reflections measured, 4320 having  $I > 2\sigma(I)$  were used in the calculations. The structure was solved by direct methods and refined by full matrix least square on all  $F^2$ . The final indices ( $I > 2\sigma(I)$ ) were  $R_1 = 0.068$ ,  $wR_2 = 0.180$ .

#### Acknowledgements

We acknowledge financial support from the Commission of European Communities (J.F.N. and M.D.V.), Conselho Nacional de Desenvolvimento Científico e Tecnológico - CNPq (M.D.V) and Fundação de Amparo à Pesquisa do Estado de São Paulo - FAPESP (M.H.A).

#### Supplementary Information

Crystallographic data (excluding structure factors) for the structures in this paper have been deposited with the Cambridge Crystallographic Data Centre as supplementary publication nos. CCDC 140420. Copies of the data can be obtained, free of charge, on application to CCDC, 12 Union Road, Cambridge CB2 1EZ, UK, (fax: +44 1223 336033 or e-mail: deposit@ccdc.cam.ac.uk).

#### References

1. Dillon, K. B.; Mathey, F.; Nixon, J. F. *Phosphorus the Carbon Copy*, John Wiley and Sons, Chichester, **1998** and references cited therein.
2. Bartsch, R.; Hitchcock, P. B.; Nixon, J. F. *J. Organomet. Chem.* **1988**, *340*, C37.

3. Müller, C.; Bartsch, R.; Fischer, A.; Jones, P. G.; Schmutzler, R. *J. Organomet. Chem.* **1996**, *512*, 141.
4. Müller, C.; Bartsch, R.; Fischer, A.; Jones, P. G. *Polyhedron* **1993**, *12*, 1383.
5. Bartsch, R.; Gelessus, A.; Hitchcock, P. B.; Nixon, J. F. *J. Organomet. Chem.* **1992**, *430*, C10.
6. Callaghan, C. S. J.; Hitchcock, P. B.; Nixon, J. F. *J. Organomet. Chem.* **1999**, *584*, 87.
7. Müller, C.; Bartsch, R.; Fischer, A.; Jones, P. G. *J. Organomet. Chem.* **1993**, *453*, C16.
8. Bartsch, R.; Gelessus, A.; Hitchcock, P. B.; Nixon, J. F. *J. Organomet. Chem.* **1992**, *430*, C10.
9. Benvenuti, M. H. A.; Hitchcock, P. B.; Nixon, J. F.; Vargas, M. D. *Chem. Commun.* **1996**, 441. Benvenuti, M. H. A.; Hitchcock, P. B.; Nixon, J. F.; Vargas, M. D. *J. Chem. Soc. Dalton Trans.* **1996**, 739.
10. Weber, L.; Sommer, O.; Stammeler, H-G.; Neumann, B.; Kölle, U. *Chem. Ber.* **1995**, *128*, 665.
11. Ajulu, F. A.; Bartsch, R.; Carmichael, D.; Johnson, J. A.; Jones, C.; Matos, R. M.; Nixon, J. F., in *Phosphorus-31 NMR Spectral Properties in Compound Characterisation and Structural Analysis*, Eds Quin, L. D. and Vekade, J. G., VCH, Weinheim, **1995**, ch. 18, pp. 229-242.
12. Braga, D.; Grepioni, F.; Byrne, J. J.; Calhorda, M. J. *J. Chem. Soc. Dalton Trans.* **1995**, 3287.
13. Besançon, K.; Laurency, G.; Lumini, T.; Roulet, R.; Gervasio, G. *Helv. Chim. Acta* **1993**, *76*, 2926 and references cited therein.
14. Lumini, T.; Laurency, G.; Roulet, R.; Tassan, A.; Ros, R.; Schenck, K.; Gervasio, G. *Helv. Chim. Acta* **1998**, *81*, 781.
15. Churchill, M. R.; Hutchinson, J. P. *Inorg. Chem.* **1978**, *17*, 3528.
16. Benvenuti, M. H. A.; Vargas, M. D.; Braga, D.; Grepioni, F.; Parisini, E.; Mann, B. E. *Organometallics*, **1993**, *12*, 2955.
17. Ros, R.; Scriveranti, A.; Albano, V. G.; Braga, D.; Garlaschelli, L. *J. Chem. Soc. Dalton Trans.* **1986**, 2411.
18. Detzel, M.; Friedrich, G.; Scherer, O. J.; Wolmershäuser, G. *Angew. Chem. Int. Ed. Engl.* **1995**, *34*, 1321.
19. Ros, R.; Scriveranti, A.; Albano, V. G.; Braga, D.; Garlaschelli, L. *J. Chem. Soc. Dalton Trans.* **1986**, 2411; Laurency, G.; Bondietti, G.; Ros, R.; Roulet, R. *Inorg. Chim. Acta* **1996**, *247*, 65 and references cited therein.
20. Bartsch, R.; Hitchcock, P. B.; Nixon, J. F. *J. Chem. Soc. Chem. Commun.* **1987**, 1146. Binger, P.; Glaser, G. *J. Organomet. Chem.* **1994**, *479*, C28.
21. Chini, P.; Ciani, G.; Garlaschelli, L.; Manassero, M.; Martinengo, S.; Sironi, A.; Canziani, F. *J. Organomet. Chem.* **1978**, *152*, C35.

Received: February 15, 2000